

Electron-electron interaction in one- and two-dimensional ferromagnetic (Ga,Mn)As

D. Neumaier,^{*} M. Schlapps, U. Wurstbauer, J. Sadowski,[†] M. Reinwald, W. Wegscheider, and D. Weiss
Institut für Experimentelle und Angewandte Physik, Universität Regensburg, 93040 Regensburg, Germany
 (Received 21 November 2007; revised manuscript received 21 December 2007; published 25 January 2008)

We investigated the magnetotransport in high quality ferromagnetic (Ga,Mn)As films and wires. At low temperature the conductivity decreases with decreasing temperature without saturation down to 20 mK. Here we show that the conductivity decrease follows a $\ln(T/T_0)$ dependency in two-dimensional films and a $-1/\sqrt{T}$ dependency in one-dimensional wires and is independent of an applied magnetic field. This behavior can be explained by the theory of electron-electron interaction.

DOI: 10.1103/PhysRevB.77.041306

PACS number(s): 73.23.-b, 75.50.Pp, 73.20.Fz

Up to now the ferromagnetic semiconductor (Ga,Mn)As (Ref. 1) is one of the best understood ferromagnetic semiconductors and has become a promising candidate for future spintronic devices. The Mn ions substituting Ga on the regular sites of the zinc-blende lattice provide both holes and magnetic moments. The ferromagnetic order between the individual Mn ions is mediated by these holes.² Ferromagnetism in (Ga,Mn)As is well understood, allowing to predict Curie temperature,² magnetocrystalline anisotropies,³ as well as anisotropic magnetoresistance effects.⁴ However, the temperature dependence of the conductivity of (Ga,Mn)As is still under debate. Starting at room temperature the conductivity decreases with decreasing temperature until a local minimum is reached around the Curie temperature. Attempts to explain this minimum include, e.g., the formation of magnetic polarons,^{5,6} or an interplay with universal conductance fluctuations.⁷ A recent work⁸ explains the temperature-dependent conductivity above and below T_C within a picture invoking localization effects using an extended version of the scaling theory of Abrahams *et al.*^{9,10} At temperatures below T_C the conductivity increases again in metallic samples, reaches a local maximum at about 10 K before it drops again for decreasing temperatures. The temperature dependence in this low-temperature regime is the focus of the present Rapid Communication. Attempts to explain this behavior are, e.g., based on Kondo scattering,¹¹ weak localization,¹² or Mott hopping.¹³ A very recent report investigating three-dimensional (3D) (Ga,Mn)As films ascribes the conductivity decrease to Aronov-Altshuler scaling in 3D.¹⁴ By using one-dimensional (1D) and two-dimensional (2D) samples we show below that the decreasing conductivity in this regime can be ascribed to electron-electron interaction (EEI). The effect of electron-electron interaction arises from a modified screening of the Coulomb potential due to the diffusive propagation.¹⁵ The expected temperature dependence of the conductivity change for EEI depends on the dimensionality and goes with $\ln(T/T_0)$ for 2D samples and with $-1/\sqrt{T}$ for 1D samples. This behavior has been found in our experiments.

For the experiment we used three different (Ga,Mn)As wafers, labeled 1–3 (see Table I), grown by low-temperature molecular beam epitaxy on semi-insulating GaAs.¹⁶ The nominal Mn concentration of the (Ga,Mn)As layers varied between 4% and 5.5% with corresponding Curie temperatures between 90 and 150 K. To investigate the transport

properties of two- and one-dimensional (Ga,Mn)As devices we fabricated Hall bars and arrays of wires using optical lithography, *e*-beam lithography, and subsequent reactive ion etching. Arrays of wires were used to suppress universal conductance fluctuations by ensemble averaging. Au contacts to the devices were made by lift-off technique. The relevant parameters of the investigated samples are listed in Table I. Magnetotransport measurements were carried out in a top-loading dilution refrigerator with a base temperature of 15 mK using standard four-probe lock-in techniques. Small measuring currents (25 pA to 1 nA) were used to avoid heating.

To investigate magnetotransport at millidegrees Kelvin temperatures, we measured the resistance of quasi-2D films and quasi-1D wires in a perpendicular applied magnetic field. According to Lee and Ramakrishnan¹⁵ a (Ga,Mn)As film is considered to be 2D in the context of electron-electron interactions if the film thickness t is smaller than the thermal diffusion length $l_T = \sqrt{\hbar D/k_B T}$. For our samples l_T is ~ 200 nm at 20 mK. Similarly, a sample is one dimensional if both wire width w and the wire thickness t are smaller than l_T .

We start with discussing temperature-dependent transport

TABLE I. Length l , width w , thickness t , and number of lines parallel N of the samples. Some of the samples were annealed for the time a at 200 °C. Curie temperature T_C , resistivity ρ , and carrier concentration p were taken on reference samples from the corresponding wafers. The screening factor F^{2D} and F^{1D} were calculated using Eq. (1) and Eq. (2), respectively. Different samples from the same wafer are labeled a, b, or c.

Sample	l_{2D}^- a	l_{2D}^- b	2_{2D}	3_{2D}	l_{1D}^- a	l_{1D}^- b	l_{1D}^- c
l (μm)	180	180	60	180	7.5	7.5	7.5
w (μm)	11	11	7.2	10	0.042	0.042	0.035
t (nm)	42	42	20	50	42	42	42
N	1	1	1	1	25	25	12
a (hours)	0	51	8.5	0	0	51	0
T_C (K)	90	150	95	90	90	150	90
p ($10^{26}/\text{m}^3$)	3.8	9.3	1.7	3.1	3.8	9.3	3.8
ρ ($10^{-5} \Omega\text{m}$)	3.5	1.8	13	5.2	3.5	1.8	3.5
F^{2D}, F^{1D}	2.4	2.4	1.8	2.6	0.76	0.72	0.80

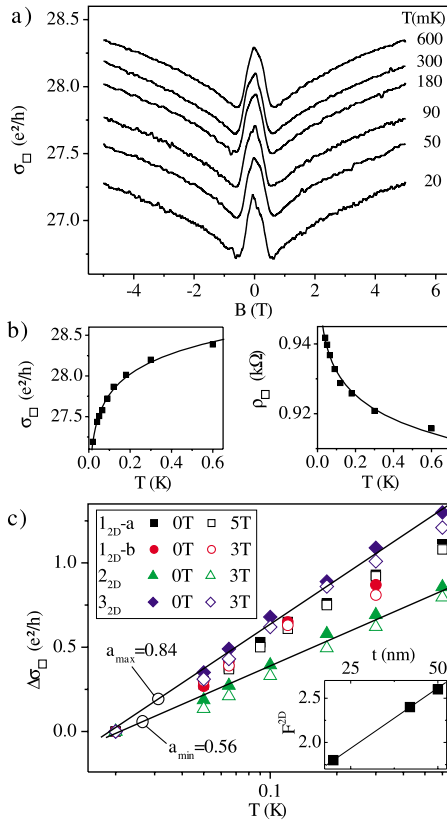


FIG. 1. (Color online) (a) Square conductivity of sample 1_{2D}-a at different temperatures in a perpendicular applied magnetic field. (b) To the left: Square conductivity at $B=0$ for different temperatures. To the right: Corresponding square resistivity at $B=0$ for different temperatures. The lines are the best $\ln(T/T_0)$ fits. (c) Change in square conductivity of the investigated 2D samples relative to 20 mK, taken at zero magnetic field (solid symbols) and $B=3$ T or $B=5$ T (open symbols). The straight lines give a slope of $a_{max}=0.84$ and $a_{min}=0.56$, which are the best linear fits for sample 3_{2D} and sample 2_{2D}, respectively. The inset shows the screening factor F^{2D} versus the (Ga,Mn)As layer thickness t .

for 2D samples (sample 1_{2D}-a, 1_{2D}-b, 2_{2D}, and 3_{2D} in Table I). The discussion for the 2D samples will be in terms of the square conductivity $\sigma_{\square}=\sigma t$, as the conductivity corrections due to electron-electron interaction are expected to be independent on the absolute value of σ_{\square} . The conductivity σ was obtained by inverting the resistivity $\rho=R(tw)/l$, with the resistance R of the investigated samples, $\sigma=1/\rho$. The square conductivity of sample 1_{2D}-a is displayed in Fig. 1(a) for temperatures between 20 and 600 mK in a perpendicular applied magnetic field B . The shape of $\sigma_{\square}(B)$ remains unchanged in this temperature range and is typical for ferromagnetic (Ga,Mn)As. The square conductivity maxima at $B=0$ stems from the anisotropic magnetoresistance⁴ (AMR) and reflects the fact that σ_{\square} for an in-plane magnetization is higher than for an out-of-plane magnetization. The positive slope of σ_{\square} for $B>400$ mT, known as negative magnetoresistance (NMR), is discussed in terms of increased magnetic order,¹⁷ or as a consequence of weak localization in three dimensions.¹² With decreasing temperature the square conductivity decreases without saturation. This behavior is also

reflected in the temperature dependence of σ_{\square} and the corresponding square resistivity $\rho_{\square}=\rho/t$ for zero magnetic field which are displayed in Fig. 1(b), respectively. This behavior is the focus of this Rapid Communication. The square conductivity change of sample 1_{2D}-a at different temperatures relative to σ_{\square} measured at 20 mK is shown in Fig. 1(c) for zero magnetic field (filled squares) and $B=5$ T (open squares). For the temperature dependence of σ_{\square} due to EEI, one obtains the following for a 2D system:¹⁵

$$\Delta\sigma_{\square} = \frac{F^{2D} e^2}{\pi h} \log_{10} \frac{T}{T_0}, \quad (1)$$

with a screening factor F^{2D} , the electron charge e , and the Planck constant h . The square conductivity change observed experimentally follows such a logarithmical temperature dependency, independent of the applied magnetic field, as it is expected from the theory of electron-electron interaction. The slope in this $\log_{10}(T)$ plot is 0.77. This corresponds to a screening factor F^{2D} of 2.4 [Eq. (1)], which is also close to the screening factor found in Co films [$F^{2D}(\text{Co})=2.0\dots2.6$].^{18,19}

Does annealing of (Ga,Mn)As change the conductivity correction? Low temperature annealing of (Ga,Mn)As causes an out diffusion of Mn ions from interstitial sites of the lattice, where they act as double donors.²⁰ Hence low-temperature annealing increases carrier concentration, square conductivity, and Curie temperature.²⁰ The relevant parameters of the annealed sample 1_{2D}-a are listed in Table I (sample 1_{2D}-b). Both carrier concentration and square conductivity increased by a factor of ~ 2 after annealing. The screening factor F^{2D} , describing the strength of EEI, however, remained unchanged, as is shown in Fig. 1(c). This demonstrates that the observed conductivity decrease is a universal phenomenon, as it is independent on the absolute value of σ_{\square} . A recent experiment of He *et al.*¹¹ seems to be in contrast to our finding. These authors observed a reduction of the logarithmical slope of the resistivity due to low-temperature annealing. If we plot for our samples instead of σ_{\square} the square resistivity change versus $\log_{10}(T)$ we obtain the same result. The change in square resistivity $\Delta\rho_{\square}$ is connected to the change in square conductivity σ_{\square} by $\Delta\rho_{\square} = 1/\sigma_{\square 1} - 1/\sigma_{\square 2} \approx \rho_{\square}^2 \Delta\sigma_{\square}$. Though $\Delta\sigma_{\square}$ remains unchanged by annealing, $\Delta\rho_{\square}$ does not. As ρ_{\square} is decreasing due to annealing, also $\Delta\rho_{\square}$ is decreasing. From the data of He *et al.*¹¹ we estimate an average screening factor F^{2D} of 2.5. This is in good agreement with our results. A monotonic dependency of the logarithmical slope and so of the screening factor F^{2D} with annealing cannot be found.

The square conductivity change of all investigated 2D samples follows a logarithmical temperature dependency and is independent of an applied magnetic field [Fig. 1(c)]. The screening factor F^{2D} of the investigated 2D samples depends on the layer thickness t . F^{2D} vs t is plotted in the lower inset of Fig. 1(c). For the investigated four samples the screening factor scales linearly with the layer thickness t . This behavior suggests that screening might play a role, although the Thomas-Fermi screening length is smaller than 1 nm and by

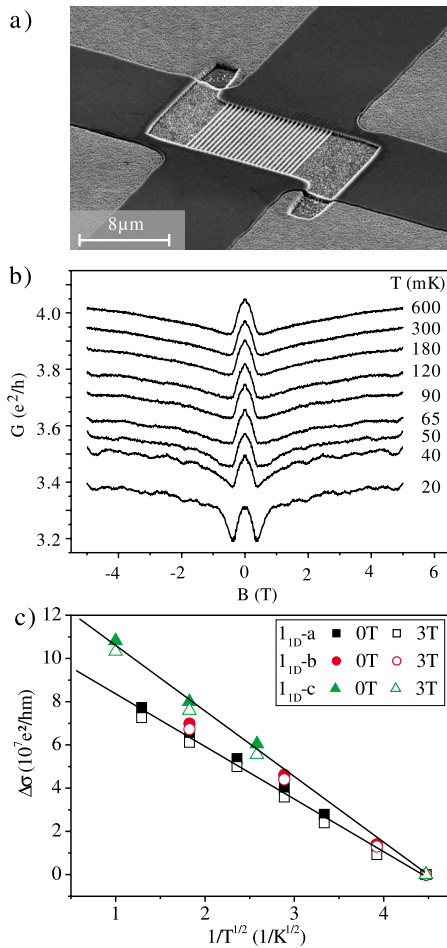


FIG. 2. (Color online) (a) Electron micrograph of sample 1_{1D} -a having 25 wires in parallel. (b) Magnetoconductance of sample 1_{1D} -a in a perpendicular applied magnetic field at different temperatures. (c) Conductivity change of the investigated 1D samples relative to 50 mK, taken at $B=0$ (solid symbols) and $B=3$ T (open symbols). The solid lines are the best linear fits for sample 1_{1D} -a and 1_{1D} -c.

this much smaller than the layer thickness t of the investigated samples (20–50 nm).

To investigate the conductivity correction in one dimension we fabricated nanowire arrays to suppress aperiodic conductance fluctuations by ensemble averaging. A corresponding electron micrograph of sample 1_{1D} -a with 25 nanowires connected in parallel is shown in Fig. 2(a). Each wire has a length l of 7.5 μm and a width w of 42 nm. The magnetoconductance of sample 1_{1D} -a is shown in Fig. 2(b) for different temperatures between 20 and 600 mK. Also for 1D samples the conductance decreases with decreasing temperature without saturation. While for $T > 50$ mK the shape of the magnetoconductance is affected by AMR and NMR, similar to the 2D samples discussed above, a weak localization correction has been found at the lowest temperatures. This weak localization in one dimension was discussed in detail in Ref. 21. Since weak localization corrections occur at temperatures < 50 mK the analysis of EEI in 1D wires is restricted to temperatures ≥ 50 mK.

The conductivity change of three 1D samples, taken relative to the conductivity at 50 mK and at zero magnetic field (filled symbols) and 3 T (open symbols), is shown in Fig. 2(c). The data points follow a $1/\sqrt{T}$ dependency independent of the applied magnetic field. Such a dependence is expected for EEI correction in 1D which is given by¹⁵

$$\Delta\sigma = -\frac{F_{1D}^{1D} e^2}{\pi A \hbar} \sqrt{\frac{\hbar D}{k_B T}}, \quad (2)$$

with a screening factor F_{1D} , the wire cross section A , the diffusion constant D , and the Boltzmann constant k_B . Again, the conductivity decrease with decreasing T can also be explained in terms of electron-electron interaction. The relevant screening factor F_{1D} [Eq. (2)] ranges between 0.72 and 0.80. Also the value of F_{1D} is close to the value found in Ni wires [$F_{1D}(\text{Ni})=0.83$].²²

We expect a dimensional crossover from 1D to 2D or 3D at temperatures above 1 K where the thermal length l_T becomes smaller than width and thickness of the wires. While data taken from sample 1_{1D} -b between 1.8 K and 8 K (not shown) are consistent with a 1D–2D transition, a $1/\sqrt{T}$ temperature dependence, expected for 1D systems, fits the data in this temperature regime equally well. A \sqrt{T} temperature dependence, expected for a 3D system, however, is not consistent with the data.

Strong spin orbit scattering, as observed in (Ga,Mn)As,²¹ affects the screening factors F^{2D} and F^{1D} but not the corresponding temperature dependence.²³ As we see no difference in the screening factor at $B=0$, where the dominating magnetic field is the spin-orbit field, and at $B=3$ T, where Zeeman splitting dominates, we conclude the effect of spin-orbit scattering on the screening factor is weak. This is consistent with previous work on Ni/(Ag,Au)/Ni films where only a weak dependence of the screening factor on spin-orbit scattering was found.²⁴

Our results obtained from 1D samples and 2D samples show that electron-electron interaction is dominating the conductance of (Ga,Mn)As in the low-temperature regime. Comparing our result with recent results of Honolka *et al.*,¹⁴ the most obvious difference is the resistivity of the investigated samples. While the resistivity of the samples investigated in Ref. 14 is $\sim 7 \times 10^{-4} \Omega\text{m}$ at 300 mK, the resistivity of our samples is between 5.5 times (sample 2_{2D}) and 40 times lower (sample 1_{2D} -b). While the devices investigated by Honolka *et al.* are already close to a metal-insulator transition, where the conductance can be described by Altshuler-Aronov scaling, we are still on the metallic side of conductance where the conductance is dominated by electron-electron interaction. The good agreement of screening factors in 1D and 2D (Ga,Mn)As samples with those found in conventional metallic ferromagnets such as Co (Refs. 18 and 19) and Ni (Ref. 22) underlines that we are on the metallic side of conductance. The mechanisms causing the conductivity decrease in both ferromagnetic semiconductor (Ga,Mn)As and ferromagnetic metals seem to be very similar. A comparable result was found by Maliepaard *et al.* in *n*-doped GaAs.²⁵

While on the metallic side conductance was dominated by electron-electron interaction, close and beyond the metal insulator transition the conductance could be described by Altshuler-Aronov scaling.

In summary we have shown that the conductivity of (Ga,Mn)As decreases with decreasing temperature below 1 K. The observed conductivity decrease in wires and films

on the metallic side of conductance can be described by EEI. The observed screening factors F_{1D} and F_{2D} are in good agreement with the screening factors found in conventional metallic ferromagnets.

We thank the German Science Foundation (DFG) for financial support via Grant No. SFB 689.

*daniel.neumaier@physik.uni-regensburg.de

[†]Present address: MAX-Laboratory, Lund University, SE-221 00, Lund, Sweden.

¹H. Ohno, *Science* **281**, 951 (1998).

²T. Dietl, H. Ohno, F. Matsukura, J. Cibert, and D. Ferrand, *Science* **287**, 1019 (2000).

³M. Sawicki, *J. Magn. Magn. Mater.* **300**, 1 (2006), and references therein.

⁴D. V. Baxter, D. Ruzmetov, J. Scherschligt, Y. Sasaki, X. Liu, J. K. Furdyna, and C. H. Mielke, *Phys. Rev. B* **65**, 212407 (2002).

⁵P. Majumdar and P. B. Littlewood, *Nature (London)* **395**, 479 (1998).

⁶M. Sawicki, T. Dietl, J. Kossut, J. Igalson, T. Wojtowicz, and W. Plesiewicz, *Phys. Rev. Lett.* **56**, 508 (1986).

⁷C. Timm, M. E. Raikh, and F. von Oppen, *Phys. Rev. Lett.* **94**, 036602 (2005).

⁸C. P. Moca, B. L. Sheu, N. Samarth, P. Schiffer, B. Janko, and G. Zarand, arXiv:0705.2016 (unpublished).

⁹E. Abrahams, P. W. Anderson, D. C. Licciardello, and T. V. Ramakrishnan, *Phys. Rev. Lett.* **42**, 673 (1979).

¹⁰G. Zarand, C. P. Moca, and B. Janko, *Phys. Rev. Lett.* **94**, 247202 (2005).

¹¹H. T. He, C. L. Yang, W. K. Ge, J. N. Wang, X. Dai, and Y. Q. Wang, *Appl. Phys. Lett.* **87**, 162506 (2005).

¹²F. Matsukura, M. Sawicki, T. Dietl, D. Chiba, and H. Ohno, *Physica E (Amsterdam)* **21**, 1032 (2004).

¹³A. Van Esch, L. Van Bockstal, J. De Boeck, G. Verbanck, A. S. van Steenberghe, P. J. Wellmann, B. Grietens, R. Bogaerts, F.

Herlach, and G. Borghs, *Phys. Rev. B* **56**, 13103 (1997).

¹⁴J. Honolka, S. Masmanidis, H. X. Tang, D. D. Awschalom, and M. L. Roukes, *Phys. Rev. B* **75**, 245310 (2007).

¹⁵P. A. Lee and T. V. Ramakrishnan, *Rev. Mod. Phys.* **57**, 287 (1985).

¹⁶M. Reinwald, U. Wurstbauer, M. Döppe, W. Kipferl, K. Wagenhuber, H.-P. Tranitz, D. Weiss, and W. Wegscheider, *J. Cryst. Growth* **278**, 690 (2005).

¹⁷E. L. Nagaev, *Phys. Rev. B* **58**, 816 (1998).

¹⁸M. Brands, A. Carl, O. Posth, and G. Dumpich, *Phys. Rev. B* **72**, 085457 (2005).

¹⁹M. Brands, C. Hassel, A. Carl, and G. Dumpich, *Phys. Rev. B* **74**, 033406 (2006).

²⁰K. W. Edmonds, P. Boguslawski, K. Y. Wang, R. P. Campion, S. N. Novikov, N. R. S. Farley, B. L. Gallagher, C. T. Foxon, M. Sawicki, T. Dietl, M. Buongiorno Nardelli, and J. Bernholc, *Phys. Rev. Lett.* **92**, 037201 (2004).

²¹D. Neumaier, K. Wagner, S. Geißler, U. Wurstbauer, J. Sadowski, W. Wegscheider, and D. Weiss, *Phys. Rev. Lett.* **99**, 116803 (2007).

²²T. Ono, Y. Ooka, S. Kasai, H. Miyajima, K. Mibu, and T. Shinjo, *J. Magn. Magn. Mater.* **226**, 1831 (2001).

²³B. L. Altshuler, A. G. Aronov, and A. Yu. Zuzin, *Solid State Commun.* **44**, 137 (1982).

²⁴J. J. Lin, S. Y. Hsu, J. C. Lue, and P. J. Sheng, *J. Phys. Chem. Solids* **62**, 1813 (2001).

²⁵M. C. Maliepaard, M. Pepper, R. Newbury, and G. Hill, *Phys. Rev. Lett.* **61**, 369 (1988).